JOURNAL OF AGRICULTURAL AND FOOD CHEMISTRY

Reactivity of Some Products Formed by the Reaction of Sorbic Acid with Sodium Nitrite: Decomposition of 1,4-Dinitro-2-methylpyrrole and Ethylnitrolic Acid

M. Teresa Pérez-Prior,[†] José A. Manso,[†] Rafael Gómez-Bombarelli,[†] Marina González-Pérez,[†] M. Pilar García-Santos,[†] Emilio Calle,[†] M. Cruz Caballero,[‡] and Julio Casado*,[†]

Departamento de Química Física, Universidad de Salamanca, E-37008 Salamanca, Spain, and Departamento de Química Orgánica, Universidad de Salamanca, E-37008 Salamanca, Spain

Sorbic acid reacts with nitrite to yield mutagenic products such as 1,4-dinitro-2-methylpyrrole (NMP) and ethylnitrolic acid (ENA). In order to know the stability of these compounds, a kinetic study of their decomposition reactions was performed in the 6.0−9.5 pH range. The conclusions drawn are as follows: (i) The decomposition of NMP occurs through a nucleophilic attack by OH^- ions, with the rate equation as follows: $r = k_{dec}^{NMP}[OH^-][NMP]$ with k_{dec}^{NMP} (37.5 °C) = 42 ± 1 M^{-1} s^{-1}. (ii) The rate law for the decomposition of ENA is as follows: $r = k_{dec}^{ENA}[ENA]K_a/(K_a + [H^+])$, with K_a being the ENA dissociation constant and k_{dec}^{ENA} (37.5 °C) = (7.11 ± 0.04) × 10^{-5} s^{-1}. (iii) The activation energies for NMP and ENA decomposition reactions are, respectively, E_a = 94 ± 3 and 94 ± 1 kJ mol^{-1}. (iv) The observed values for the decomposition rate constants of NMP and ENA in the pH range of the stomach lining cells, into which these species can diffuse, are so slow that they could be the slow determining step of the alkylation mechanisms by some of the products resulting from NMP and ENA decomposition. Thus, the current kinetic results are consistent with the low mutagenicity of these species.

KEYWORDS: Nitrite; sorbic acid; 1,4-dinitro-2-methylpyrrole; ethylnitrolic acid.

INTRODUCTION

Sorbic acid (*trans,trans*-2,4-hexadienoic acid) and its potassium, sodium, and calcium salts are used as preservatives in a wide range of foodstuffs, such as cheese, pickles, sauces, and wine. They inhibit the growth of fungi and yeasts and have antibacterial activity (*1*). Accordingly, many analytical methods have been proposed to determine the amount of sorbic acid and sorbates in different types of samples (*2, 3*). Sorbates have been reported to be more efficient and less toxic than benzoate (*4*) and are classified as "*Generally Recognized as Safe*" (GRAS) additives by the U.S. Food and Drug Administration (FDA) (*5*). Nevertheless, a weak genotoxic potential of stored sorbate solutions has been reported (*6*−*11*). In light of this, the alkylating potential of the sorbic acid has been investigated previously (*12, 13*).

Nitrite is widely used in the curing of meat, where, in conjunction with sodium chloride, it inhibits the growth and toxin production of *Clostridium botulinum* (*14*). Since the discovery in 1956 that nitrosamines are powerful carcinogens, there has been a noteworthy increase in studies addressing nitrosamine chemistry, in particular the formation and reactions of these substances. This area continues to be one of major concern, since nitrosamines can readily be formed under acidic conditions (e.g., in the human stomach) from many naturally occurring amines and ingested nitrate and nitrite (*15*−*17*).

Because sorbic acid also inhibits *Clostridium botulinum* growth as well as the formation of nitrosamines, it has been proposed as a partial replacement for nitrite in meat curing. However, this practice may lead to other toxicological problems since sorbic acid reacts with nitrite to yield certain mutagenic products (*18*) (**Scheme 1**). The main mutagens seem to be 1,4-dinitro-2-methylpyrrole (NMP) and ethylnitrolic acid (ENA) (*19*).

Since (i) a comparison of the alkylating capacity of NMP and ENA with their mutagenic potential could be of interest and (ii) knowledge of the kinetic parameters of the decomposition reactions of those species (and, hence, of their stability) is

Scheme 1. Reaction of Sorbic Acid with Sodium Nitrite

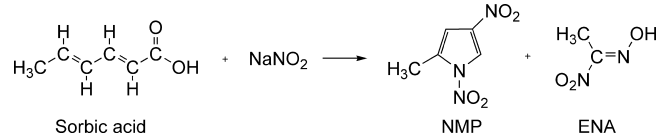

* To whom correspondence should be addressed. E-mail: jucali@usal.es. Tel.: +34 923 294486. Fax: +34 923 294574.
[†] Departamento de Química Física, Universidad de Salamanca.
[‡] Departamento de Química Orgánica, Universidad de Salamanca.

10.1021/jf802822y CCC: $40.75
Published on Web 11/18/2008

Scheme 2. Decomposition Reaction of 1,4-Dinitro-2-methylpyrrole

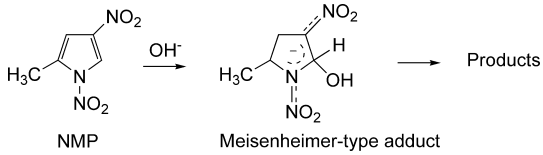

Scheme 3. Decomposition Reaction of Ethylnitrolic Acid (ENA) Present in Its Nondissociated (HA) and Dissociated (A^-) Forms

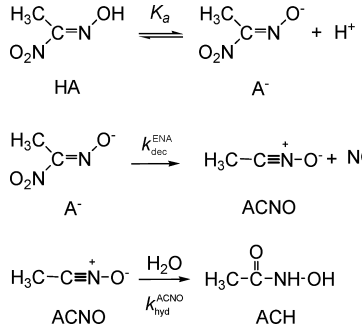

necessary as a previous step in the investigation of their alkylating potential, here we were prompted to address this issue.

MATERIALS AND METHODS

To monitor the NMP and ENA decomposition reactions (**Schemes 2** and **3**), their absorbances at the wavelengths of maximum absorption (λ = 269 nm and λ = 328 nm, respectively) were followed. The hydrolysis reaction of acetonitrile oxide (ACNO) was monitored spectrophotometrically at λ = 210 nm, where the product acetohydroxamic acid (ACH) absorbs. A Shimadzu UV-2401-PC spectrophotometer with a thermoelectric six-cell holder temperature control system (±0.1 °C) was used. Detailed reaction conditions are given in the figure and table legends.

Reactions were carried out in the 6.0−9.5 pH range. Phosphate and borate buffers were used to maintain constant pH. A Crison Micro pH 2000 pH-meter was used for pH measurements (±0.01). The reaction temperature was kept constant (±0.05 °C) with a Lauda Ecoline RE120 thermostat.

Titrations were performed using a pH-Stat Metrohm 718 STAT Titrino, which releases NaOH, previously normalized with potassium hydrogen phthalate. An QSTAR XL TOF-MS system (Applied Biosystems) was used for the determination of accurate masses. NMR proton spectra were obtained with a Varian spectrometer Mod. Mercury VS2000 (200 MHz).

Water was deionized with a MilliQ-Gradient (Millipore). Sorbic acid and sodium nitrite were from Panreac. Nitroethane and D_2O (98%) were obtained from Aldrich.

All kinetic runs were performed in triplicate. Numerical treatment of the data was performed using the 7.1.44 Data Fit software.

Procedures: Synthesis of 1,4-Dinitro-2-methylpyrrole and Ethylnitrolic Acid. 1,4-Dinitro-2-methylpyrrole was obtained from the reaction between sorbic acid and sodium nitrite in aqueous solution at pH = 3.5 (*18, 20*). A solution of sodium nitrite (11.0 g) was added to a partially suspended solution of sorbic acid (2.2 g) in distilled water (200 mL). Keeping the pH of the mixture constant at 3.5 with dilute H_2SO_4, the mixture was stirred at 60 °C for 2 h. The mixture was extracted with four 50 mL portions of CH_2Cl_2. The combined extracts were washed with water, dried over Na_2SO_4, and evaporated to dryness in vacuo to give the residue. The residue was recrystallized in chloroform ether.

UV λ_{max} in nm (ε, M^{-1} cm^{-1}): 209 (11621 ± 123), 229 (17428 ± 135), 270 (13551 ± 107), 329 (8764 ± 66), 385 (1806 ± 19). ^1H NMR ($CDCl_3$): δ 2.64 (s, 3H, CH_3), 7.9 (d, 1H, CH−C−NO_2), 8.8 (d, 1H, CH−N−NO_2). Accurate mass calculated for $C_5H_5N_3O_4Na$ (M^+Na): 194.017227; Found: 194.0187.

Ethylnitrolic acid was obtained from the nitrosation reaction of nitroethane in acidic aqueous solution. Sodium nitrite (8.9 g) was added to a solution of nitroethane (8 mL) in aqueous sodium hydroxide (4.3 g in 100 mL) at 0 °C. Simultaneously to sodium nitrite addition, a solution of sulfuric acid (5 M) was slowly added to maintain an acidic pH in the reaction mixture. The aqueous solution was extracted with three 50 mL portions of ether and evaporated to dryness in vacuo to give the product. The product was recrystallized in dichloromethane hexane. Because of its low thermal stability, it was stored at 0 °C.

UV λ_{max} in nm (ε, M^{-1} cm^{-1}): 240 (4341 ± 29) in acid media and 328 (8237 ± 17) in alkaline medium. ^1H NMR ($CDCl_3$): δ 2.46 (s, 3H, CH_3), 9.3 (broad, 1H, OH).

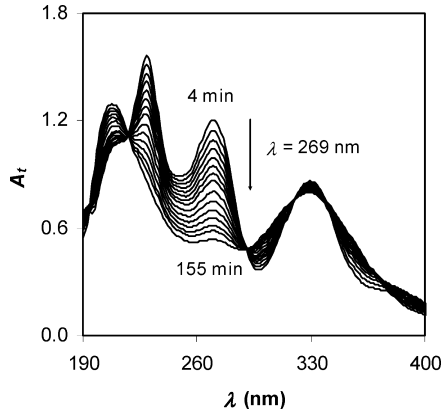

Figure 1. Spectra showing the NMP decomposition over time: $[NMP]_o = 10^{-4}$ M; T = 32.5 °C; pH = 9.47 with borate buffer.

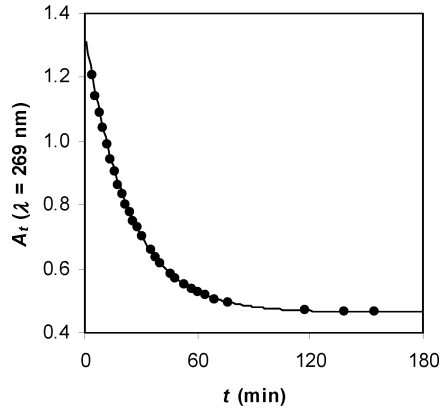

Figure 2. Determination of k_{obs}^{NMP} (eq 3): $[NMP]_o = 10^{-4}$ M; T = 32.5 °C; pH = 9.47 with borate buffer.

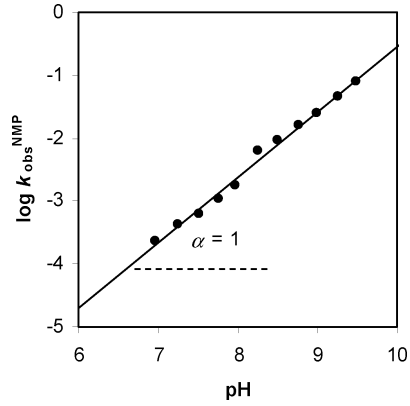

Figure 3. Variation in the NMP decomposition rate constant with the acidity of the medium at T = 37.5 °C: $[NMP]_o = 10^{-4}$ M; phosphate and borate buffers.

RESULTS AND DISCUSSION

Decomposition of 1,4-Dinitro-2-methylpyrrole. 1,4-Dinitro-2-methylpyrrole undergoes decomposition, and an inverse

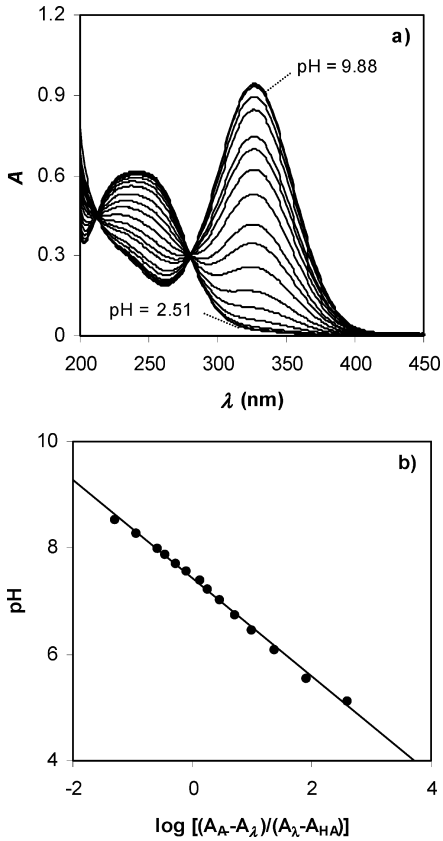

Figure 4. (a) Absorption spectra of ENA at different pH's and (b) determination of the pK_a of ENA in water at 25.0 °C (eq 4): $[ENA]_o = 1.4 \times 10^{-4}$ M; $\lambda = 350$ nm.

kinetic isotope effect, $k^{NMP}_{dec\ H_2O}/k^{NMP}_{dec\ D_2O} = 0.7$, was observed. This result was interpreted in terms of a nucleophilic attack of the OH^- on the NMP molecule. Since OD^- is a stronger nucleophile than OH^-, the direct nucleophilic attack on the electrophilic carbon (**Scheme 2**) would be expected to proceed faster in D_2O (*21*), as was observed.

The presence of nitro groups on the pyrrole ring may play a significant role in lowering the high π-electron density of the ring and in favoring the attack of the nucleophilic reagent (*20, 22*). This explains the formation of the Meisenheimer-type adduct due to the addition of OH^- on the NMP molecule.

The following rate equation was observed for NMP decomposition,

$$r = -\frac{d[NMP]}{dt} = k^{NMP}_{dec}[OH^-][NMP] = k^{NMP}_{obs}[NMP] \quad (1)$$

where k^{NMP}_{obs} is the pseudofirst-order rate constant:

$$k^{NMP}_{obs} = k^{NMP}_{dec}[OH^-] \quad (2)$$

By designating the absorbance values of NMP as A_o, A_t, and A_∞ at times, respectively, zero, t, and infinity (end of the reaction), integration of eq 1 yields eq 3:

$$A_t = A_\infty + (A_o - A_\infty)e^{-k^{NMP}_{obs}t} \quad (3)$$

Figure 1 depicts the variation in the absorption of NMP with time. **Figure 2** shows a typical kinetic run for the decomposition reaction of NMP in aqueous solution.

Experiments were performed at different pH's (**Figure 3**), with the slope $\alpha = 1$ revealing first order with respect to the concentration of OH^- (eq 2).

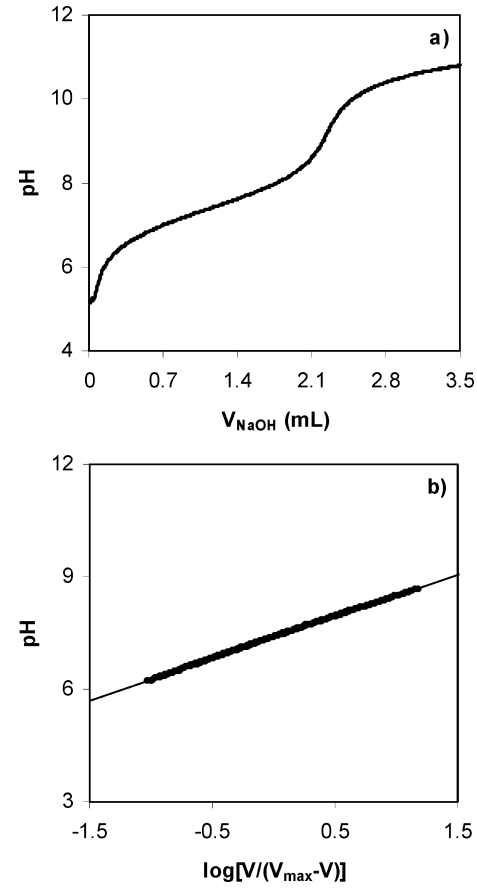

Figure 5. (a) Titration curve for ENA and (b) determination of the pK_a of ENA in water at 25.0 °C (eq 5): $[ENA]_o = 2 \times 10^{-3}$ M; [NaOH] = 9.38 $\times 10^{-2}$ M.

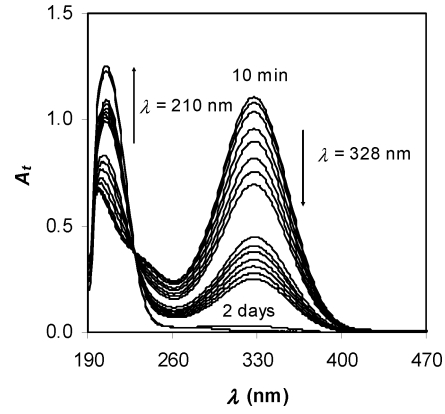

Figure 6. Spectrograms showing the variation in ENA absorbance at different times: $[ENA]_o = 1.3 \times 10^{-4}$ M; $T = 32.5$ °C; pH = 9.52 with borate buffer.

By fitting the absorbance values against those of time (eq 3), the rate constant k^{NMP}_{obs} was found to be k^{NMP}_{obs} ($T = 32.5$ °C) = $(7.22 \pm 0.05) \times 10^{-4}$ s^{-1} at pH 9.47. Using eq 2, at different pH values, the NMP decomposition rate constant was found to be k^{NMP}_{dec} ($T = 32.5$ °C) = 22 ± 1 M^{-1} s^{-1}. The values of k^{NMP}_{dec} at different temperatures are reported in **Table 1**.

Decomposition of Ethylnitrolic Acid. Since (i) the stability of ethylnitrolic acid decreases with increasing pH and (ii) the dissociated acid molecule undergoes NO_2^- loss, this being the limiting step (*23*), the mechanism shown in **Scheme 3** for the decomposition of ENA was investigated.

Because (i) all the kinetic experiences were carried out in the pH = 6−9.5 range and (ii) the ACH pK_a = 9.31 (*24, 25*)

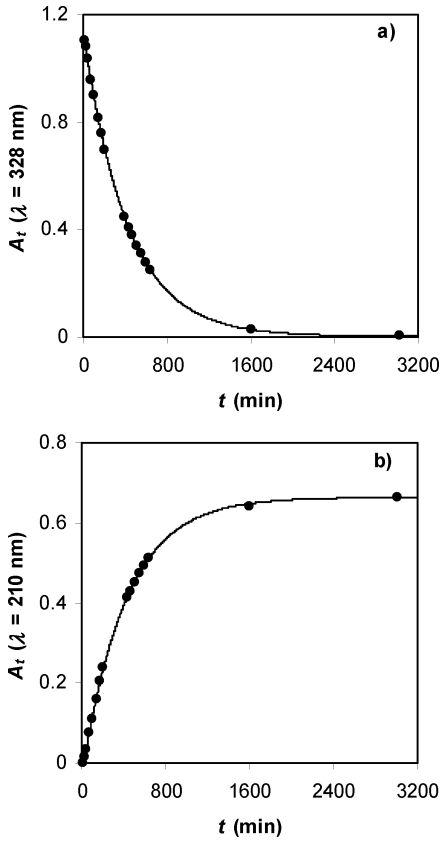

Figure 7. (a) Determination of k_{obs}^{ENA} (eq 8) and (b) k_{obs}^{ACNO} (eq 11): $[ENA]_o = 1.3 \times 10^{-4}$ M; $T = 32.5$ °C; pH = 9.52 with borate buffer.

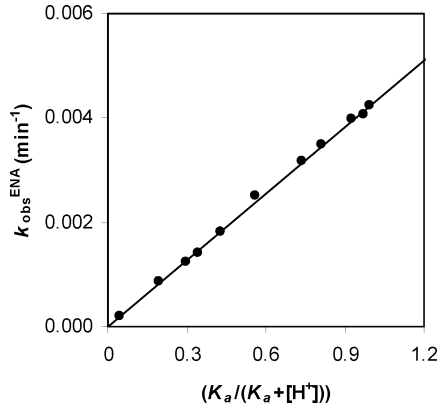

Figure 8. Variation of k_{obs}^{ENA} with $K_a/(K_a + [H^+])$ (eq 8): $[ENA]_o = 10^{-4}$ M; $T = 37.5$ °C; $K_a = 4 \times 10^{-8}$ M.

(in water at 25 °C), it can be assumed that all the ACH is protonated in the working acidity range. To determine k_{dec}^{ENA} and k_{hyd}^{ACNO}, the value of the equilibrium constant K_a was determined by spectrometric and titration methods.

Determination of the Ethylnitrolic Acid Dissociation Constant. *(a) Spectrometric Method.* **Figure 4a** shows the UV−vis absorption spectra for ENA at several pH's, with a well-defined isosbestic point at $\lambda = 282$ nm. It may be observed that the undissociated (HA) and dissociated (A^-) forms of ENA show maximum absorption at 240 and 328 nm, respectively. Since at $\lambda = 350$ nm the absorption of the anion is maximum and that of the neutral ethylnitrolic acid is practically null, we studied the equilibrium at this wavelength. Spectra were obtained at pH 2−10, and the absorbance/pH data were fitted using the Henderson−Hasselbalch equation (*26*),

$$pH = pK_a + \log\frac{[A^-]}{[HA]} = pK_a - \log\frac{A_{A^-} - A_\lambda}{A_\lambda - A_{HA}} \quad (4)$$

where A_{HA} and A_{A^-}, respectively, represent the absorbances of the nondissociated ($\lambda = 350$ nm, pH ≈ 2) and totally dissociated ($\lambda = 350$ nm, pH ≈ 10) forms of ENA. A_λ represents the absorbance values at pH's between these boundary limits at $\lambda = 350$ nm.

Figure 4b shows the good fit of the results to the Henderson−Hasselbalch equation ($\lambda = 350$ nm) and gives the value $K_a = (4 \pm 1) \times 10^{-8}$ M for the ENA dissociation constant ($T = 25.0$ °C).

(b) Titrimetric Method. By measuring the sodium hydroxide consumed for the titration of ENA at different pH values with a pH-Stat, the Henderson−Hasselbalch equation can be applied in the form

$$pH = pK_a + \log\frac{V}{V_{max} - V} \quad (5)$$

where V_{max} represents the volume of NaOH at the end point and V is the volume of NaOH used at any other point during the titration. Parts a and b of **Figure 5**, respectively, show the titration curve and the Henderson−Hasselbalch plot, which gives the value $K_a = (4 \pm 1) \times 10^{-8}$ M for the ENA dissociation constant ($T = 25.0$ °C).

In light of the results of both the spectrometric and titrimetric measurements for the ethylnitrolic acid dissociation constant, we used the value $K_a = (4 \pm 1) \times 10^{-8}$ M (variation in the K_a value in the temperature range where the kinetic experiments were performed is smaller than the experimental error with which K_a was determined).

Determination of the k_{dec}^{ENA} and k_{hyd}^{ACNO} Rate Constants. Since the ethylnitrolic acid concentration [ENA] can be expressed as the sum of the concentration of nondissociated ethylnitrolic acid (HA) plus that present as anion (A^-),

$$[ENA] = [HA] + [A^-] \quad (6)$$

and because $K_a = ([A^-][H^+]/[HA])$, eq 7 is readily deduced from **Scheme 3**,

$$r = -\frac{d[ENA]}{dt} = k_{dec}^{ENA}\frac{K_a}{K_a + [H^+]}[ENA] = k_{obs}^{ENA}[ENA] \quad (7)$$

where k_{obs}^{ENA} is the pseudofirst-order rate constant:

$$k_{obs}^{ENA} = k_{dec}^{ENA}\frac{K_a}{K_a + [H^+]} \quad (8)$$

By designating the absorbance values of ENA as A_o, A_t, and A_∞ at times, respectively, zero, t, and infinity (end of the reaction), the integration of eq 7 yields eq 9:

$$A_t = A_\infty + (A_o - A_\infty)e^{-k_{obs}^{ENA}t} \quad (9)$$

Figure 6 shows the variation in the absorption of ENA with time.

Figure 7a represents a typical kinetic run for the decomposition reaction of ENA in aqueous solution.

By fitting the absorbance values against those of time (eq 9), the rate constant was found to be k_{obs}^{ENA} ($T = 32.5$ °C) = $(3.96 \pm 0.03) \times 10^{-5}$ s^{-1} at pH = 9.52. Using eq 8, ENA decomposition rate constant was found to be k_{dec}^{ENA} ($T = 32.5$ °C) = $(3.99 \pm 0.03) \times 10^{-5}$ s^{-1}.

Table 1. Rate Constants as a Function of Temperature for the Decomposition Reactions of 1,4-Dinitro-2-methylpyrrole and Ethylnitrolic Acid[a]

	NMP	ENA	
T (°C)	k_{dec}^{NMP} (M^{-1} s^{-1})[a]	10^5 k_{dec}^{ENA} (s^{-1})	10^5 k_{hyd}^{ACNO} (M^{-1} s^{-1})
25.0	9.4 ± 0.5	1.53 ± 0.03	0.6 ± 0.2
27.5	11.9 ± 0.9	2.17 ± 0.05	0.9 ± 0.2
30.0	17.2 ± 0.6	2.86 ± 0.04	1.2 ± 0.4
32.5	22 ± 1	3.99 ± 0.03	1.4 ± 0.4
35.0	32 ± 1	5.31 ± 0.04	1.8 ± 0.6
37.5	42 ± 1	7.11 ± 0.04	2.1 ± 0.1

[a] Values are given within the 95% confidence interval.

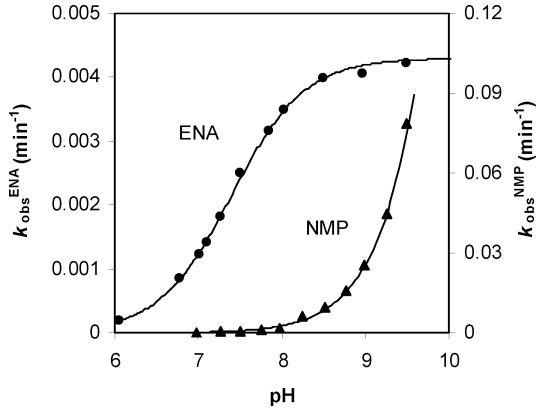

Figure 9. Variation in k_{obs}^{NMP}(▲) and k_{obs}^{ENA}(●) decomposition rate constants (see **Schemes 2** and **3**) with pH: $[NMP]_o = [ENA]_o = 10^{-4}$ M; $T = 37.5$ °C.

According to the above mechanism, the rate equation for the formation of acetohydroxamic acid (ACH) is given by eq 10:

$$r = \frac{d[ACH]}{dt} = k_{hyd}^{ACNO}[ACNO][H_2O] = k_{obs}^{ACNO}[ACNO] \quad (10)$$

[ACNO] is the acetonitrile oxide concentration at time t and k_{obs}^{ACNO} is the pseudofirst-order hydrolysis rate constant, defined as follows:

$$k_{obs}^{ACNO} = k_{hyd}^{ACNO}[H_2O] \quad (11)$$

According to the general kinetic scheme for consecutive first-order reactions (*27*) and the boundary condition $[ACNO]_o = 0$, the concentration of acetonitrile oxide at time t is given by eq 12:

$$[ACNO] = \frac{k_{obs}^{ENA}[ENA]_o}{k_{obs}^{ACNO} - k_{obs}^{ENA}}(e^{-k_{obs}^{ENA}t} - e^{-k_{obs}^{ACNO}t}) \quad (12)$$

Integration of eq 10 and expression of the result in terms of absorbance leads to the following,

$$A_t = \varepsilon_{ACH} l [ENA]_o \left(1 + \frac{k_{obs}^{ENA} e^{-k_{obs}^{ACNO}t} - k_{obs}^{ACNO} e^{-k_{obs}^{ENA}t}}{k_{obs}^{ACNO} - k_{obs}^{ENA}}\right) \quad (13)$$

where A_t is the absorbance of acetohydroxamic acid at time t, ε_{ACH} is the absorption coefficient of this species, and l is the light path.

Figure 7b shows the good fit of the experimental results to eq 13, which allows, with the above calculated value of k_{obs}^{ENA}, the pseudofirst-order hydrolysis rate constant to be determined: k_{obs}^{ACNO} ($T = 32.5$ °C) = (7.7 ± 0.2) × 10^{-4} s^{-1}. With this value, eq 11 immediately affords that of k_{hyd}^{ACNO} ($T = 32.5$ °C) = (1.4 ± 0.4) × 10^{-5} M^{-1} s^{-1}. The values of k_{hyd}^{ACNO} at different temperatures are reported in **Table 1**.

With the previously determined K_a and k_{obs}^{ENA} values, eq 8 allows one to know the value of the decomposition rate constant k_{dec}^{ENA} (see **Scheme 3**). **Figure 8** shows the good fit of the experimental results to that equation, with the slope of the plot being the value of k_{dec}^{ENA}.

Since the influence of the pH of the reaction medium in the decomposition rate constants of NMP and ENA is quantitatively measured by $k_{obs}^{NMP}$and k_{obs}^{ENA}, the values of these constants were plotted against those of pH (**Figure 9**). Because the alkylating potential of NMP and ENA (which is currently being investigated by us) were measured at neutral pH—as in the stomach-lining cells into which such products can diffuse—the plot represented in **Figure 9** reveals that, in the vicinity of neutral pH, the values of the decomposition rate constants $k_{obs}^{NMP}$and k_{obs}^{ENA} are small (e.g., for ENA, the reaction half-time is $\tau_{1/2} \approx 12$ h). Although definitive conclusions cannot be drawn until later studies allow us to know the alkylation rate constants by NMP and ENA, the current results do show that the decomposition reactions of these species formed in the reaction of sorbic acid with sodium nitrite are so slow that they could be the slow determining step of the alkylation mechanisms by some of the mutagenic products resulting from NMP and ENA decomposition (*18, 28*). Thus, the present kinetic approach is consistent with the low mutagenicity of NMP and ENA. In any case, further experimental work is necessary to check the possible existence of a correlation between the chemical reactivity of NMP/ENA and their mutagenicity, as has been demonstrated with other alkylating agents such as lactones (*29−31*).

With the k_{dec}^{NMP}, k_{dec}^{ENA}, and k_{hyd}^{ACNO} values reported in **Table 1**, the following energies of activation were obtained for the respective reactions: E_a (decomposition of NMP) = 94 ± 3 kJ mol^{-1}; E_a (decomposition of ENA) = 94 ± 1 kJ mol^{-1}; and E_a (hydrolysis of ACNO) = 73 ± 5 kJ mol^{-1}.

From the present study, the following conclusions may be drawn:

(1) The decomposition of NMP occurs through a nucleophilic attack by OH^- ions, with the rate equation being the following: $r = k_{dec}^{NMP}[OH^-][NMP]$ with k_{dec}^{NMP} (37.5 °C) = 42 ± 1 M^{-1} s^{-1}.

(2) The rate law for the decomposition of ENA is as follows: $r = k_{dec}^{ENA}$ $[ENA]K_a/(K_a + [H^+])$, with K_a being the ENA dissociation constant and k_{dec}^{ENA} (37.5 °C) = (7.11 ± 0.04) × 10^{-5} s^{-1}.

(3) The activation energies for NMP and ENA decomposition reactions are, respectively, $E_a = 94 \pm 3$ and 94 ± 1 kJ mol^{-1}.

(4) The observed values for the decomposition rate constants of NMP and ENA in the pH range of stomach-lining cells, into which these species can diffuse, are so slow that they could be the slow determining step of the alkylation mechanisms by some of the products resulting from NMP and ENA decomposition. Thus, the current kinetic results are consistent with the low mutagenicity of these species.

ACKNOWLEDGMENT

We thank the Spanish Ministerio de Ciencia e Innovación (CTQ2007-63263), as well as the Spanish Junta de Castilla y León (Grant SA040 A08) for supporting the research reported in this article. M.T.P.P., J.A.M., and M.G.P. thank the Junta de Castilla y León, for Ph.D. grants. R.G.B. thanks the Ministerio

de Ciencia e Innovación for Ph.D. grant. Thanks are also given for the valuable comments made by the referees.

LITERATURE CITED

(1) Hasegawa, M. M.; Nishi, Y.; Ohkawa, Y.; Inui, N. Effects of Sorbic Acid and its Salts on Chromosome Aberrations, Sister Chromatid Exchanges and Gene Mutations in Cultured Chinese Hamster Cells. *Food Chem. Toxicol.* **1984**, *22*, 501–507.

(2) Schripsema, J. Comprehensive Analysis of Polar and Apolar Constituents of Butter and Margarine by Nuclear Magnetic Resonance, Reflecting Quality and Production Processes. *J. Agric. Food Chem.* **2008**, *56*, 2547–2552.

(3) Horiyama, S.; Honda, C.; Suwa, K.; Umemoto, Y.; Okada, Y.; Semma, M.; Ichikawa, A.; Takayama, M. Sensitive and Simple Analysis of Sorbic Acid Using Liquid Chromatography with Electrospray Ionization Tandem Mass Spectrometry. *Chem. Pharm. Bull.* **2008**, *56*, 578–581.

(4) Thakur, B. R.; Singh, K.; Arya, S. S. Chemistry of Sorbates—A Basic Perspective. *Food Rev. Int.* **1994**, *10*, 71–91.

(5) *U.S. Food and Drug Administration, Center for Food Safety and Applied Nutrition. FDA List of Food Additives that are Generally Recognized as Safe (GRAS)*; U.S. GPO: Washington, DC, 2005.

(6) Münzer, R.; Guigas, C.; Renner, H. W. Reexamination of Potassium Sorbate and Sodium Sorbate for Possible Genotoxic Potential. *Food Chem. Toxicol.* **1990**, *28*, 397–401.

(7) Würgler, F. E.; Schlatter, J.; Maier, P. The Genotoxicity Status of Sorbic Acid, Potassium Sorbate and Sodium Sorbate. *Mutat. Res.* **1992**, *283*, 107–111.

(8) Fritsch, P.; Cassand, P.; de Saint Blanquat, G. Genotoxicity Study of Reaction Products of Sorbic Acid. *J. Agric. Food Chem.* **2000**, *48*, 3605–3610.

(9) Mpountoukas, P.; Vantarakis, A.; Sivridis, E.; Lialiaris, T. Cytogenetic Study in Cultured Human Lymphocytes Treated with Three Commonly Used Preservatives. *Food Chem. Toxicol.* **2008**, *46*, 2390–2393.

(10) Schlatter, J.; Würgler, F. E.; Kränzlin, R.; Maier, P.; Holliger, E.; Graf, U. The Potential Genotoxicity of Sorbates—Effects on Cell-Cycle in Vitro in V79 Cells and Somatic Mutations in Drosophila. *Food Chem. Toxicol.* **1992**, *30*, 843–851.

(11) Schiffmann, D.; Schlatter, J. Genotoxicity and Cell-Transformation Studies with Sorbates in Syrian-Hamster Embryo Fibroblasts. *Food Chem. Toxicol.* **1992**, *30*, 669–672.

(12) Pérez Prior, M. T.; Manso, J. A.; García Santos, M. P.; Calle, E.; Casado, J. Alkylating Potential of Potassium Sorbate. *J. Agric. Food Chem.* **2005**, *53*, 10244–10247.

(13) Pérez Prior, M. T.; Manso, J. A.; García Santos, M. P.; Calle, E.; Casado, J. Sorbic Acid as an Alkylating Agent. *J. Solution Chem.* **2008**, *37*, 459–466.

(14) Adams, J. B. Food Additive−Additive Interactions involving Sulphur Dioxide and Ascorbic and Nitrous Acids: A Review. *Food Chem.* **1997**, *59*, 401–409.

(15) Williams, D. L. H. *Nitrosation*; Cambridge University Press: Cambridge, U.K., 1988.

(16) Casado, J. Nitrosation Reactions. Invited Lecture. In *Fast Reactions in Solution*; Royal Society of Chemistry Annual Meeting, Burgos, Spain, 1994.

(17) Walker, R. Nitrates, Nitrites and *N*-Nitrosocompounds: A Review of the Occurrence in Food and Diet and the Toxicological Implications. *Food Addit. Contam.* **1990**, *7*, 717–768.

(18) Namiki, M.; Osawa, T.; Ishibashi, H.; Namiki, K.; Tsuji, K. Chemical Aspects of Mutagen Formation by Sorbic Acid−Sodium Nitrite Reaction. *J. Agric. Food. Chem.* **1981**, *29*, 407–411.

(19) Osawa, T.; Namiki, M. Mutagen Formation in the Reaction of Nitrite with the Food Components Analogous to Sorbic Acid. *Agric. Biol. Chem.* **1982**, *46*, 2299–2304.

(20) Kito, Y.; Namiki, M.; Tsuji, K. A New *N*-Nitropyrrole. 1,4-Dinitro-2-methylpyrrole, Formed by the Reaction of Sorbic Acid with Sodium Nitrite. *Tetrahedron* **1978**, *34*, 505–508.

(21) Brown, R. S.; Bennet, A. J.; Ślebocka-Tilk, H. Recent Perspectives Concerning the Mechanism of H_3O^+- and OH^--Promoted Amide Hydrolysis. *Acc. Chem. Res.* **1992**, *25*, 481–488.

(22) de Santis, F.; Stegel, F. Interaction between Dinitropyrroles and Methoxide Ion: An NMR Study. *Tetrahedron Lett.* **1974**, 1079–1080.

(23) Egan, E.; Clery, M.; Hegarty, A. F.; Welch, A. J. Mechanism of Reaction of Isomeric Nitrolic Acids to Nitrile Oxides in Aqueous Solution. *J. Chem. Soc., Perkin Trans. 2* **1991**, 249–256.

(24) Senent, M. L.; Niño, A.; Muñoz-Caro, C.; Ibeas, S.; García, B.; Leal, J. M.; Secco, F.; Venturini, M. Deprotonation Sites of Acetohydroxamic Acid Isomers. A Theoretical and Experimental Study. *J. Org. Chem.* **2003**, *68*, 6535–6542.

(25) Mora-Diez, N.; Senent, M. L.; García, B. Ab Initio Study of Solvent Effects on the Acetohydroxamic Acid Deprotonation Processes. *Chem. Phys.* **2005**, *324*, 350–358.

(26) Po, H. N.; Senozan, N. M. The Henderson−Hasselbalch Equation: Its History and Limitations. *J. Chem. Educ.* **2001**, *78*, 1499–1503.

(27) Connors, K. A. *Chemical Kinetics. The Study of Reaction Rates in Solution*; VCH: New York: 1990; Chapter 3.

(28) Namiki, M.; Udaka, S.; Osawa, T.; Tsuji, K.; Kada, T. Formation of Mutagens by Sorbic Acid−Nitrite Reaction: Effects of Reaction Conditions on Biological Activities. *Mutat. Res.* **1980**, *73*, 21–28.

(29) Pérez Prior, M. T.; Manso, J. A.; García Santos, M. P.; Calle, E.; Casado, J. Reactivity of Lactones and GBH Formation. *J. Org. Chem.* **2005**, *70*, 420–426.

(30) Manso, J. A.; Pérez Prior, M. T.; García Santos, M. P.; Calle, E.; Casado, J. A Kinetic Approach to the Alkylating Potential of Carcinogenic Lactones. *Chem. Res. Toxicol.* **2005**, *18*, 1161–1166.

(31) Gómez Bombarelli, R.; González Pérez, M.; Pérez Prior, M. T.; Manso, J. A.; Calle, E.; Casado, J. Chemical Reactivity and Biological Activity of Diketene. *Chem. Res. Toxicol.* **2008**, *21*, 1964–1969.

Received for review September 11, 2008. Revised manuscript received October 29, 2008. Accepted October 30, 2008.

JF802822Y